Proceedings of the IMECE 2017 Conference
IMECE 2017
November 3-9, 2017, Tampa, Florida

IMECE2017-70206

MECHANISMS UNDERLYING RAPID ELECTRONUCLEATION AND FREEZING OF HYDRATES

Palash V. Acharya
Department of Mechanical Engineering
The University of Texas at Austin
Austin, Texas, USA

Arjang Shahriari
Department of Mechanical Engineering
The University of Texas at Austin
Austin, Texas, USA

Denise Lin
Department of Mechanical Engineering
The University of Texas at Austin
Austin, Texas, USA

Vaibhav Bahadur*
Department of Mechanical Engineering,
Texas Materials Institute
The University of Texas at Austin
Austin, Texas, USA

ABSTRACT

Nucleation of hydrates is constrained by very long induction (wait) times, which can range from hours to days. Electronucleation (application of an electrical potential across the precursor solution) can significantly reduce the induction time for nucleation. This study shows that porous aluminum foams (open-cell) enable near-instantaneous electronucleation at very low voltages. Experiments with tetrahydrofuran hydrates reveal that aluminum foam electrodes enable voltage-dependent nucleation with induction times of only tens of seconds at voltages as low as 20 V. Foam-based electrodes can reduce the induction time by up to 150X when compared to non-foam electrodes. Furthermore, this study reveals that electronucleation can be attributed to two distinct phenomena, namely bubble generation (due to electrolysis), and the formation of metal-ion coordination compounds. These mechanisms affect the induction time to different extents and depend on electrode material and polarity. Overall, this work uncovers the benefits of using foams for formation of hydrates, with foams aiding nucleation as well as propagation of the hydrate formation front.

*Corresponding author: vb@austin.utexas.edu

INTRODUCTION

Clathrate hydrates [1, 2] are water-based solids with a guest molecule trapped in a lattice of water molecules. Hydrates have significant potential in applications such as storage and transportation of natural gas [1,4,5]. Other applications include CO_2 capture and sequestration, hydrate based desalination, and hydrogen storage etc. [1-5]. The formation of many hydrates like methane hydrates in laboratory conditions is hindered by high pressure and low-temperature requirements. Furthermore, hydrate formation requires significant induction time, which can range from hours to days, especially in quiescent systems [3]. This presents challenges for the development of applications [4, 5], requiring rapid hydrate formation (e.g. natural gas transportation by forming a hydrate). The use of surfactants and mechanical agitation of the precursor solution are common techniques to promote the formation of hydrates [6, 7].

The present group recently demonstrated electronucleation for rapid and controlled nucleation of hydrates [10]. Experiments with Tetrahydrofuran (THF) hydrate formation demonstrated a significant reduction in induction time on the application of electrical potentials using stainless steel (inert) electrodes dipped in the precursor solution. The voltage-dependent induction time was reduced [10] to a few minutes at high voltages (100 V).

The present study reveals that aluminum foam-based electronucleation electrodes can reduce the induction time by more than 150X when compared to bare stainless steel electrodes. The use of aluminum foams for hydrate formation has been previously explored [11, 12] to enable rapid removal of the heat generated during hydrate formation. This study shows that aluminum foams also accelerate the nucleation kinetics, which can be attributed to two separate phenomena (bubble generation, and formation of aluminum-based metal-ion complexes). These mechanisms are strongly dependent on the material and polarity of the electrodes. Importantly, aluminum

foam electrodes trigger near-instantaneous nucleation when used as the anode. Induction times on the order of 10 seconds were observed at low voltages of 20 V, which is a significant advancement over previous work [10]. Overall, this work studies the electrochemistry-based mechanisms and analyzes the benefits of foam-based electro-nucleation.

EXPERIMENTAL DETAILS

THF hydrates were used in the present study as a substitute for methane hydrates [13-16], since they are easier to form. THF forms hydrates from a THF-water mixture (molar ratio of THF:water is 1:17) at atmospheric pressure, and below 4.4 °C. A slight excess of THF was used in this work to prevent ice formation.

A schematic of the experimental setup is shown in Figure 1. Experiments were conducted in a cold isothermal bath, with a 50/50 mixture of ethylene glycol and water. Electronucleation was studied in 14 mm diameter glass tubes fitted with a rubber stopper to prevent evaporation, and hold the two electrodes and a T-type ungrounded thermocouple.

Open-cell aluminum foams with 92 % porosity and a surface area-to-volume of 1720 m^2/m^3 were used. A 6 mm x 8 mm x 50 mm sized foam plug was used as the electrode. A stainless steel electrode was the other electrode. The spacing between the electrodes and thermocouple was 5 mm. The electrodes were connected to a DC power supply and an ammeter. Additionally, baseline experiments were conducted with two stainless steel electrodes.

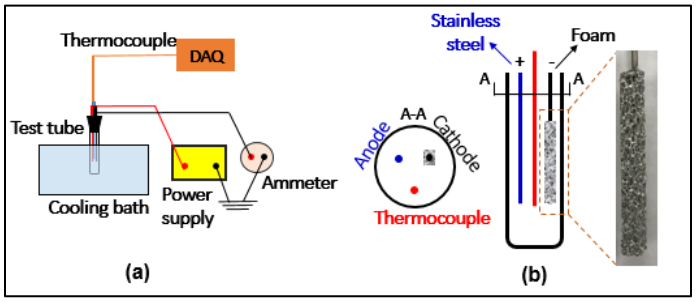

Figure 1. (a) Schematic of experimental setup, (b) Stainless steel and aluminum foam electrodes inside the tube.

A tube containing the water-THF mixture was agitated and degassed in a sonication bath. The tube was immersed in the bath at 5 °C, till it reached steady state. The bath temperature was then lowered to -5 °C. Once the contents of the tube reached -5 °C, an electrical voltage was applied. The induction time was measured from this point onwards to the time when hydrates nucleated.

Electronucleation was detected by tracking the thermal signature of the solution, as detailed in our previous study [10]. The heat released at the onset of nucleation instantaneously raises the temperature of the solution to ~ 4 °C (Figure 2). Another indication [10] of hydrate nucleation is a sudden decrease in the electrical conductivity due to the formation of hydrates (Figure 2). Similar techniques have previously been used to infer the nucleation of THF hydrates [17] and ice [18-20].

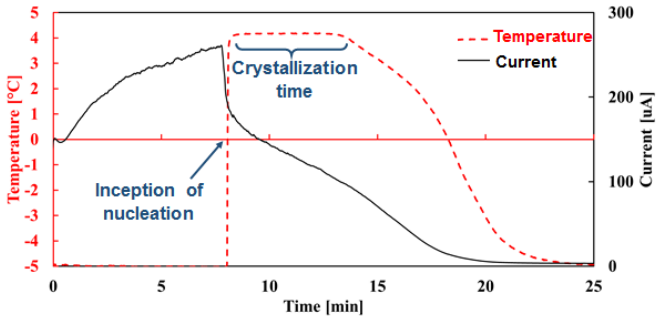

Figure 2. Temperature and current flow in the precursor hydrate forming solution. The onset of nucleation is accompanied by a rise in the temperature along with a simultaneous decrease in current flow.

RESULTS AND DISCUSSIONS

Figure 3 shows the measured induction time versus the voltage for the baseline (non-foam) case and the cases with the aluminum foam electrode as the cathode/anode. Each data point is the average of more than five individual measurements. The baseline case, showed a voltage-dependent reduction in the induction time, as per our previous study [10]. Aluminum foam as the cathode (negative polarity) significantly reduced the induction time. This highlights the benefits of foams, with the high surface area of the foams clearly promoting nucleation (the foam provided a 17X enhancement in the surface area, as compared to the bare electrode).

The induction time can be further reduced (Figure 3), by using the foam electrode as the anode (positive polarity). At 5 V, the induction time is reduced by 40X when compared to the foam as the cathode. The average induction times at 10 V and 20 V were only 43 seconds and 20 seconds, respectively. This is a substantial increase in nucleation kinetics when compared with our previous work [10]. Positively biased aluminum electrodes can enable instantaneous nucleation, which will benefit applications needing 'hydrates on demand'. It is noteworthy that no nucleation was observed in any experiment at 0 V even after twelve hours. Overall, these results suggest that aluminum foams as the anode can enable > 100X reduction in induction time as compared to non-foam inert electrodes. It is noted that data used in Figure 3 is tabulated in Table 1.

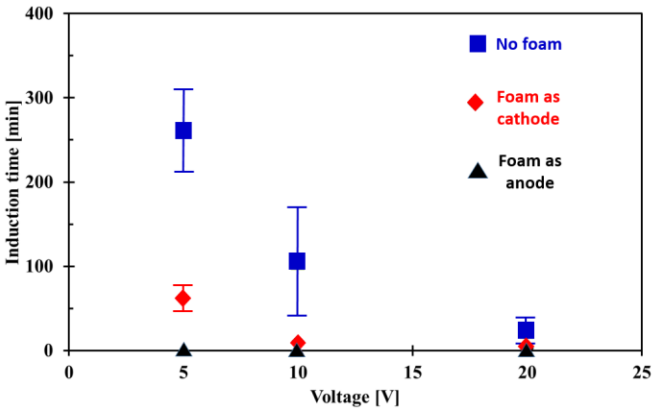

Figure 3. Induction time versus voltage for the baseline (non-foam) case, and the cases where the aluminum foam is the cathode/anode.

Table 1: Induction time (in minutes)

	Al foam as cathode				Al foam as anode			
Voltage (V)	**20**	**10**	**5**	**0**	**20**	**10**	**5**	**0**
Average	2.1	10.2	62	>12 hours	0.3	0.7	1.6	>12 hours
Standard deviation	0.3	1.9	7	-	0.1	0.16	0.3	-

	Non-foam electrodes			
Voltage (V)	**20**	**10**	**5**	**0**
Average	21.8	103.6	280.9	>12 hours
Standard deviation	13.8	65.7	27.9	-

	Al foam as cathode	
Voltage (V)	50	80
Average	0.59	0.35
Std. Dev	0.2	0.18

The influence of polarity on electronucleation is significant. The above experiments show that the induction time reduced by 40X, 14X, and 7X at 5, 10, and 20V respectively, by switching the polarity of the foam to be the anode. Furthermore, experiments with Al foam as cathode at higher voltages suggest that very high voltages (>80 V) would be required to obtain the induction times resulting from using Al foam as an anode at low voltages (~20V). This suggests that utilizing Al foam as an anode can significantly reduce the supercooling requirements, which would benefit many energy-related applications.

Polarity-dependent induction times indicate that multiple physical phenomena are likely at play. One possible mechanism briefly mentioned in our previous study [10] was bubble generation at the electrodes, resulting from hydrolysis. These bubbles act as nucleation sites, and the convection associated with bubble growth and detachment can trigger nucleation. Bubble generation on the foam electrode was indeed observed, as described below.

This study identifies another mechanism, which affects nucleation more strongly than bubble-related effects, and is polarity dependent. It has been hypothesized [22-25] that the electrofreezing enhancement of water can be attributed to the formation of aluminum-based coordination compounds at the electrodes, the structure of which resembles the structure of ice [22]. This mechanism is analyzed in this work to explain accelerated hydrate formation with aluminum foam anode.

Both the above mechanisms and the related chemical reactions are discussed in detail. For foam electrode as the cathode, water is reduced to hydroxyl ions and hydrogen gas is generated (Figure 4a), which accounts for the bubbles ($4H_2O + 4e^- \rightarrow 4OH^- + 2H_2\uparrow$) at the cathode. The high surface area of the foam, and the presence of nucleation sites (bubbles) explains the faster electronucleation as compared to the non-foam electrode. At the anode (stainless steel) the hydroxyl ions are oxidized to generate oxygen ($4OH^- \rightarrow O_2\uparrow + 2H_2O + 4e^-$). Importantly, Joule heating is very low in these experiments. Also, stoichiometric calculations indicate that less than 0.001 % of water is hydrolyzed.

Polarity-dependent nucleation is explained by a different reaction when the foam is the anode. Oxidation of aluminum is favored [22] over the oxidation of hydroxyl ions. Al^{3+} ions enter the solution and are surrounded by water molecules to form a hydroxo-aquo-aluminum coordination compound $[Al(H_2O)_6]^{3+}$. Furthermore, OH^- ions form bridges between the coordination compounds leading to the synthesis of an octahedral polynuclear complex [22] (Figure 4b). We believe (like in [22]), that the resemblance of this structure to the structure of the hydrate promotes nucleation. Furthermore, since the physics of the nucleation is primarily determined by the number of oxidized or hydrolyzed ions, it is the magnitude of the applied voltage, translating into the number of ions entering the precursor solution rather the electric field itself, which will be the key factor underlying electronucleation.

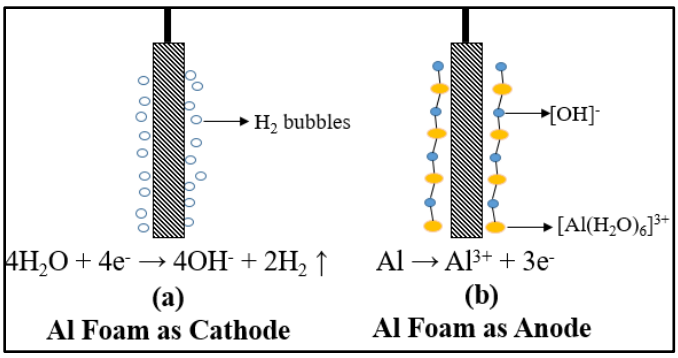

Figure 4. Mechanisms underlying electronucleation (a) Bubble-related effects with foam as cathode (b) Coordination compound formation-based nucleation with foam as anode.

The bubble formation mechanism was validated by visualization of bubbles in the foam electrode. When the foam is the cathode, significant bubble generation is seen on the foam (Figure 5a). Effects associated with bubble growth and detachment can provide the activation energy for nucleation.

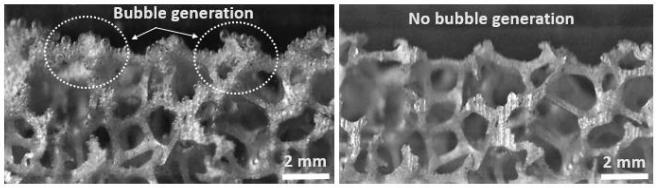

Figure 5. Aluminum foams as (a) cathode, leading to bubble generation, and (b) anode, (no bubbles observed).

There is no bubble generation when the foam is the anode (Figure 5b). This indicates that an alternative reaction (oxidation of aluminum) occurs at the foam anode, and is responsible for nucleation promotion. It is noted that it is challenging to experimentally detect coordination compounds at the interface. This work detected Al^{3+} ions in solution, which are the precursors to these coordination compounds.

The current-time plot (Figure 1c) can be used to estimate the concentration of Al^{3+} ions in the present experiments, by estimating the total charge transfer in the solution till the onset of nucleation. The molar concentrations have been summarized in Table 2. These calculations indicate that the concentrations of Al^{3+} ions will be (O) 10^{-6} mol/liter at the onset of nucleation. The resulting $[Al(H_2O)_6]^{3+}$ concentrations would be challenging to detect with conventional spectroscopic studies [26-28].

Table 2. Molar concentration of Al ions in the solution at the onset of nucleation.

	Al Foam as Anode		
Voltage (V)	20	10	5
Concentration (x 10^{-6} mol/L)	1.92	1.77	1.66

In this work, a colorimetric indicator reaction was used to show that Al^{3+} ions enter the solution when the foam is the anode. Pyrocatechol Violet (PV) is used as a complexometric indicator dye to detect the presence of Group III cations [29-31]. PV was used to detect Al^{3+} ions in solution. Figure 6 shows the foam electrode as the cathode and the anode in separate experiments where 0.2 mM PV is dissolved in the solution. With the foam as the cathode (Figure 6a), no color change is seen (there is bubble formation, which will also accelerate nucleation). However, when the foam is anode (Figure 6b) the color of the solution changes to violet-blue as the PV chelates aluminum ions.

The above experiments attribute accelerated hydrate nucleation to the formation of aluminum-based coordination compound. Induction time measurements indicate that this mechanism influences nucleation more strongly than bubble-related effects.

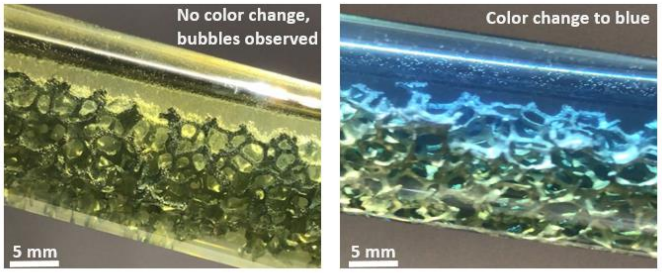

Figure 6. Bubble generation (a) on the foam as the cathode. However, when the foam is the anode, there is a color change (b), which indicates that aluminum ions enter the solution to form aluminum-based coordination compounds, which accelerate electronucleation.

BENEFITS OF FOAMS IN HYDRATE FORMATION

Metal foams also accelerate the rate at which the hydrate formation front progresses, in addition to promoting electronucleation. This is due to the higher thermal conductivity (~12 W/mK) when compared to the conductivity of the precursor solution alone (0.6 W/mK). Higher thermal conductivity aids removal of the heat generated during formation. The effective thermal conductivity of a metal foam ($k_{effective}$) in a liquid is [32]:

$$k_{effective} = k_{Al}\left[\frac{2+\frac{k_{sol}}{k_{Al}}-2\emptyset\left(1-\frac{k_{sol}}{k_{Al}}\right)}{2+\frac{k_{sol}}{k_{Al}}+\emptyset\left(1-\frac{k_{sol}}{k_{Al}}\right)}\right] \quad (1)$$

where k_{Al} is thermal conductivity of aluminum, k_{sol} is thermal conductivity of the THF/water solution and $\emptyset$ is the foam porosity.

The decreased time for hydrate formation was quantified by measuring the phase change propagation time (time since the onset of nucleation to convert the entire tube to a hydrate plug). This can be inferred from the temperature-time curve in Figure 1c and is summarized for in Table 3. The propagation time for the -5°C experiments is reduced from 7.5 minutes (non-foam electrodes used) to 5.1 minutes with the foam (average of 5 experiments with the foam as the cathode and anode). The foam polarity and the voltage magnitude did not influence the propagation time. Repeating the experiments at -10°C shows that

the propagation time is reduced from 4.8 minutes to 1.9 minutes with foams. It should be carefully noted that that hydrate formation is determined by all the pathways available to reject heat; the present results apply only to this geometry. Overall, it is clear that the heat transfer benefits and the electronucleation promotion resulting with foams will assist in the synthesis of hydrates.

Table 3. Time taken for hydrates to form in the entire tube (minutes).

Bath temperature	With foam electrode	Without foam electrode
-5°C	5.1	7.5
-10°C	1.9	4.8

CONCLUSIONS

In conclusion, this study reveals that positively biased aluminum foams can enable near-instantaneous low voltage electronucleation. This study has shown up to a 150X decrease in induction time with foams, as compared to non-foam cases. Bubble-based mechanistic effects and electrochemistry-based mechanisms influence the nucleation kinetics. While this study used THF hydrates, similar benefits are possible for other hydrate systems such as cyclopentane and methane hydrates. Overall this work shows that foam-based electronucleation can promote rapid hydrate formation without excessive supercooling, which has energy consumption reduction benefits.

ACKNOWLEDGEMENTS

The authors acknowledge American Chemical Society Petroleum Research Fund PRF 54706- DNI5, Welch Foundation Grant # F-1837 and National Science Foundation grant CBET-1653412 for supporting this work.

REFERENCES

[1] Eslamimanesh, A.; Mohammadi, A. H.; Richon, D.; Naidoo, P.; Ramjugernath, D. Application of Gas Hydrate Formation in Separation Processes: A Review of Experimental Studies. J. Chem. Thermodyn. 2012, 46, 62−71.

[2] Veluswamy, H. P.; Kumar, R.; Linga, P. Hydrogen Storage in Clathrate Hydrates: Current State of the Art and Future Directions. Appl. Energy 2014, 122, 112−132.

[3] Sloan, E.D. and Koh, C.A., Clathrate Hydrates of Natural Gases Third Edition. CRC Press, **2008**, *119*.

[4] Sum, A. K.; Koh, C. A.; Sloan, E. D. Clathrate Hydrates: From Laboratory Science to Engineering Practice. Ind. Eng. Chem. Res. **2009**, 48 (16), 7457–7465.

[5] Chatti, I.; Delahaye, A.; Fournaison, L.; Petitet, J. P. Benefits and Drawbacks of Clathrate Hydrates: A Review of Their Areas of Interest. Energy Convers. Manag. **2004**, 46, 1333–134.

[6] Zhong, Y.; Rogers, R. E. Surfactant Effects on Gas Hydrate Formation. Chem. Eng. Sci. **2000**, 55, 4175–4187.

[7] Zhang, J. S.; Lee, S.; Lee, J. W. Kinetics of Methane Hydrate Formation from SDS Solution. Ind. Eng. Chem. Res. **2007**, 46, 6353−6359.

[8] Ganji, H.; Manteghian, M.; Sadaghiani zadeh, K.; Omidkhah, M. R.; Rahimi Mofrad, H. Effect of Different Surfactants on Methane Hydrate Formation Rate, Stability and Storage Capacity. Fuel **2007**, 86, 434−441.

[9] Ando, N.; Kuwabara, Y.; Mori, Y. H. Surfactant Effects on Hydrate Formation in an Unstirred Gas/liquid System: An Experimental Study Using Methane and Micelle-Forming Surfactants. Chem. Eng. Sci. **2012**, 73, 79−85.

[10] Carpenter K.; Bahadur V.; Electronucleation for rapid and controlled formation of hydrates. J. Phys. Chem. Lett., **2016** , 7(13) , 2465-2469

[11] Yang L.; Fan S.S.; Wang Y.H.; Lang X.M; Xie D.L. Accelerated formation of methane hydrate in aluminum foam. Ind. Eng. Chem., **2011** , 50 , 11563-11569.

[12] Fan, S., Yang, L., Lang, X., Wang, Y., and Xie, D., 2012, "Kinetics and thermal analysis of methane hydrate formation in aluminum foam," Chem. Eng. Sci., 82, pp. 185–193

[13] Wilson, P. W.; Lester, D.; Haymet, a. D. J. Heterogeneous Nucleation of Clathrates from Supercooled Tetrahydrofuran (THF)/water Mixtures, and the Effect of an Added Catalyst. Chem. Eng. Sci. **2005**, 60, 2937–2941.

[14] Zhang, J. S.; Lo, C.; Somasundaran, P.; Lu, S.; Couzis, A.; Lee, J. W. Adsorption of Sodium Dodecyl Sulfate at THF Hydrate / Liquid Interface. J. Phys. Chem. **2008**, 112, 12381–12385.

[15] Liu, W.; Wang, S.; Yang, M.; Song, Y.; Wang, S.; Zhao, J. Investigation of the Induction Time for THF Hydrate Formation in Porous Media. J. Nat. Gas Sci. Eng. **2015**, 24, 357–364.

[16] Wilson, P. W.; Haymet, A. D. J. Hydrate Formation and Re-Formation in Nucleating THF/water Mixtures Show No Evidence to Support a "Memory" Effect. Chem. Eng. J. **2010**, 161, 146−150.

[17] Tombari, E.; Presto, S.; Salvetti, G.; Johari, G. P. Heat Capacity of Tetrahydrofuran Clathrate Hydrate and of Its Components, and the Clathrate Formation from Supercooled Melt. J. Chem. Phys. **2006**, 124, 154507−154506.

[18] Dai, S.; Lee, J. Y.; Santamarina, J. C. Hydrate Nucleation

in Quiescent and Dynamic Conditions. Fluid Phase Equilib. **2014**, 378, 107−112.

[19] Bauerecker, S.; Ulbig, P.; Buch, V.; Vrbka, L.; Jungwirth, P. Monitoring Ice Nucleation in Pure and Salty Water via High-Speed Imaging and Computer Simulations. J. Phys. Chem. C **2008**, 167, 7631−7636.

[20] Alizadeh, A.; Yamada, M.; Li, R.; Shang, W.; Otta, S.; Zhong, S.; Ge, L.; Dhinojwala, A.; Conway, K. R.; Bahadur, V.; et al. Dynamics of Ice Nucleation on Water Repellent Surfaces. Langmuir **2012**, 28 , 3180−3186.

[21] Carpenter, K.; Bahadur, V. Electrofreezing of Water Droplets under Electrowetting Fields. Langmuir **2015**, 31, 2243–2248.

[22] Hozumi T.; Saito A.; Okawa S.; Watanabe K. Effects of electrode materials on freezing of supercooled water in electric freeze control. Int. J. Refrig., **2003**, 26, 537-542.

[23] Shichiri T.; Nagata T. Effect of Electric currents on the nucleation of ice crystals in the melt. J. Cryst. Growth, **1981,** *54* ,207-210

[24] Orlowska M.; Havet M; Le-Bail A. Controlled ice nucleation under high voltage DC Electrostatic field conditions. FoodRes. Int., **2009** , 42(7), 879-884.

[25] Wei S.; Xiaobin X.; Hong Z,; Chuanxiang X. Effect of dipole polarization of water molecules on ice formation under an electrostatic field. Cryobiology, **2008**, 56, 93-99.

[26] Hay, M.B. and Myneni, S.C., Geometric and Electronic Structure of the Aqueous $[Al(H_2O)_6]^{3+}$ Complex., The Journal of Physical Chemistry A, **2008,** *112*(42), pp.10595-10603

[27] Hay, M.B. and Myneni, S.C., X-ray absorption spectroscopy of aqueous aluminum-organic complexes, The Journal of Physical Chemistry A, **2010,** *114*(20), pp.6138-6148.

[28] Rudolph, W.W., Mason, R. and Pye, C.C. Aluminium (III) hydration in aqueous solution. A Raman spectroscopic investigation and an ab initio molecular orbital study of aluminium (III) water clusters, *Physical Chemistry Chemical Physics*, **2000**, *2*(22), pp.5030-5040.

[29] Narin I.; Tuzen M.; Soylak M. Aluminium determination in environmental samples by graphite furnace atomic absorption spectrometry after solid phase extraction on Amberlite XAD-1180/pyrocatechol violet chelating resin. Talanta, **2004**, 63, 411-418.

[30] Marczenko Z. Separation and Spectrophotometric Determination of Elements, Wiley, Chichester, **1986**.

[31] Narin I.; Soylak M.; Elci L.; Dogan M. Determination of trace metal ions by AAS in natural water samples after preconcentration of pyrocatechol violet complexes on an activated carbon column. Talanta, **2000**, 52, 1041-1046.

[32] Reay, D.; Kew, P. Heat pipes theory, design and applications (5th ed.). Oxford, UK: Butterworth-Heinemann, **2006.**